Inorg. Chem. **2005**, *44*, 2753–2760

Temperature Dependence of the Crystal Structure and *g*-Values of $[(HC(Ph_2PO)_3)_2Cu](ClO_4)_2 \cdot 2H_2O$: Influence of Dynamic Jahn–Teller Coupling and Lattice Strain Interactions

Charles J. Simmons,*,† Horst Stratemeier,‡ Graeme R. Hanson,§ and Michael A. Hitchman‡

Division of Natural Sciences, University of Hawaii at Hilo, Hilo, Hawaii 96720-4091, School of Chemistry, University of Tasmania, Box 252-75 Hobart, TAS 7001, Australia, and Centre for Magnetic Resonance, University of Queensland, St. Lucia, QLD 4072, Australia

Received October 7, 2004

The temperature dependence of the X-ray crystal structure and powder EPR spectrum of $[(HC(Ph_2PO)_3)_2Cu](ClO_4)_2 \cdot 2H_2O$ is reported, and the structure at room temperature confirms that reported previously. Below ~100 K, the data imply a geometry with near elongated tetragonal symmetry for the $[(HC(Ph_2PO)_3)_2Cu]^{2+}$ complex, but on warming the two higher Cu–O bond lengths and *g*-values progressively converge, and by 340 K the bond lengths correspond to a compressed tetragonal geometry. The data may be interpreted satisfactorily assuming an equilibrium among the energy levels of a $Cu–O_6$ polyhedron subjected to Jahn–Teller vibronic coupling and a lattice strain. However, agreement with the experiment is obtained only if the orthorhombic component of the lattice strain decreases to a negligible value as the temperature approaches 340 K.

Introduction

The coordination geometry of six-coordinate copper(II) complexes is strongly influenced by Jahn−Teller (JT) vibronic coupling.[1] Because the JT active vibration is doubly degenerate, the JT distortion may produce a geometry of either tetragonal or orthorhombic symmetry. For six identical ligands, a tetragonally elongated octahedral geometry is the most stable,[2] with each pair of trans Cu−ligand bonds being equally likely to undergo elongation. However, in crystal sites of tetragonal or lower symmetry, lattice forces will stabilize a form in which the axial elongation occurs to one particular pair of ligand atoms, at the same time inducing an orthorhombic distortion.[3] If these lattice forces are weak, a form in which the long axis distorts toward a different pair of ligand atoms may be only slightly higher in energy. Thermal population of this higher-energy form may then occur, and the geometry observed by X-ray crystallography at high temperatures will not be the local geometry of the copper(II) complex.[4] This has sometimes led to incorrect conclusions being drawn concerning the geometry of a copper(II) complex, with it being identified as the unusual, compressed tetragonal form,[5] when in reality it is the common orthorhombically distorted, tetragonally elongated octahedron, but with the direction of the long axis disordered over two directions.[6]

Disorder of the above kind may be identified by analysis of the thermal ellipsoid parameters of the atoms,[7] though this is sometimes difficult and careful comparison with the analogous complex of a non-JT-active metal ion is usually required.[8] Extended X-ray absorption fine structure (EXAFS)[9] has proved a useful method of determining the local bond lengths in compounds of this kind.[10] The determination

* Author to whom correspondence should be addressed. E-mail: simmonsc@hawaii.edu.
† University of Hawaii at Hilo.
‡ University of Tasmania.
§ University of Queensland.

(1) Hathaway, B. J. *Struct. Bonding (Berlin)* **1984**, *57*, 55.
(2) (a) Reinen, D.; Atanasov, M. *Magn. Reson. Rev.* **1991**, *15*, 167. (b) Deeth, R. J.; Hitchman, M. A. *Inorg. Chem.* **1986**, *25*, 1225.
(3) Hitchman, M. A. *Comments Inorg. Chem.* **1994**, *15*, 197.
(4) Simmons, C. J. *New J. Chem.* **1993**, *17*, 77.
(5) Tucker, D.; White, P. S.; Trojan, K. L.; Kirk, M. L.; Hatfield, W. E. *Inorg. Chem.* **1991**, *30*, 823.
(6) Stratemeier, H.; Wagner, B.; Krausz, E. R.; Linder, R.; Schmitke, H.-H.; Pebler, J.; Hatfield, W. E.; ter Haar, L.; Reinen, D.; Hitchman, M. A. *Inorg. Chem.* **1994**, *33*, 2320.
(7) Trueblood, K. N.; Dunitz, J. D. *Acta Crystallogr., Sect. B* **1983**, *39*, 120.
(8) (a) Ammeter, J. H.; Bürgi, H. B.; Gamp, E.; Meyer-Sandrin, V.; Jensen, W. P. *Inorg. Chem.* **1979**, *18*, 733. (b) Stebler, B.; Bürgi, H.-B. *J. Am. Chem. Soc.* **1987**, *109*, 1395. (c) Tregenna-Piggott, P. L. W.; Andres, H. P.; McIntyre, G. J.; Best, S. P.; Wilson, C. C.; Cowan, J. A. *Inorg. Chem.* **2003**, *42*, 1350.
(9) Zhang, H. H.; Hedman, B.; Hodgson, K. O. In *Inorganic Electronic Structure and Spectroscopy*; Solomon, E. I., Lever, A. B. P., Eds.; Wiley: New York, 1999; Vol. 1, Chapter 9.

10.1021/ic048604h CCC: $30.25
Published on Web 03/17/2005

of X-ray crystal structures over a temperature range has also been valuable in this respect, because the variation of the bond lengths mirrors the change in thermal population of the structural forms.[4] We have developed a theoretical model to calculate the geometry and *g*-values of a copper(II) complex under the influence of JT coupling and a lattice strain[11,12] and have applied this to the interpretation of a range of compounds exhibiting temperature-dependent electron paramagnetic resonance (EPR) spectra and/or crystal structures.[13−15] The model has the advantage that it provides detailed information on the potential surface of the complex, the lattice interactions, and, on occasion, features such as cooperative interactions between the complexes.[16]

The crystal structure of the complex $[(HC(Ph_2PO)_3)_2Cu](ClO_4)_2 \cdot 2H_2O$ at 298 K yielded bond lengths [2.132 (×2), 2.157 (×2), 1.977 (×2) Å] which suggest the unusual tetragonally compressed geometry, and initially the results were interpreted in this way.[17] However, the EXAFS of the compound at room temperature[18] indicated Cu−O distances consistent with the more common tetragonally elongated geometry [1.96 (×4), 2.22 (×2) Å], implying that the X-ray data were influenced by disorder. To investigate whether the disorder is caused by a dynamic JT effect and, if this is the case, to provide detailed information on the lattice interactions in the compound, the crystal structure and EPR spectrum of the compound have been measured over a wide temperature range. The present paper reports the results of this study.

Experimental Results

Preparation of $[(HC(Ph_2PO)_3)_2Cu](ClO_4)_2 \cdot 2H_2O$. The experimental procedure reported by Shieh et al.[17] did not work. The following alternative procedure was developed. An acetone (36 mL) solution containing 1.999 g (3.5 mmol) of the ligand tris-(diphenylphosphino)methane, $HC(Ph_2P)_3$ or tdpm (Alpha Products, Johnson-Matthey), was stirred at 0 °C for 40 min. Then 1.21 g of the oxidizing agent, H_2O_2 (30% solution) dissolved in 12 mL of acetone, was added dropwise to the tdpm solution for 40 min, and the resulting reaction mixture was stirred on ice for 2 h and at room temperature for one more hour. The solution was filtered and left to precipitate in distilled H_2O overnight. Then it was filtered and dried *in-vacuo* at ∼80 °C. The resulting product consisted of whitish and brownish-white powders with a yield of ∼45%. [Observed (brownish powder): C, 68.0; H, 5.1. Observed (whitish powder): C, 69.2; H, 4.7. Calculated for $HC(Ph_2PO)_3$ or $C_{37}H_{31}O_3P_3$: C, 72.8; H, 5.1.] The disagreement in analysis is probably due to hydration. The oxidized ligand, $HC(Ph_2PO)_3$ or tdpom (0.3658 g, 0.59 mmol), was then dissolved in 40 mL of warm (∼70 °C) 1-butanol, and to this mixture was added a solution of 0.1064 g of high-purity $Cu(H_2O)_6(ClO_4)_2$ (0.29 mmol) dissolved in 10 mL of deionized H_2O. The resulting reaction mixture turned milky white; it was clarified by adding an extra 100 mL of warm 1-butanol followed by 20 mL of H_2O and further heating. The clear, warm solution was left to evaporate slowly for several days and then was filtered, yielding beautiful white, transparent crystals containing mainly $[(HC(Ph_2PO)_3)_2Cu](ClO_4)_2 \cdot 2H_2O$. (Observed: C, 58.0; H, 4.2. Calculated for $C_{74}H_{66}Cl_2CuO_{16}P_6$: C, 58.0; H, 4.3.) Although the unit cell parameters of most crystals matched those reported by Shieh et al.[17] for triclinic $[(HC(Ph_2PO)_3)_2Cu](ClO_4)_2 \cdot 2H_2O$, a few crystals were monoclinic: $a = 12.622$ Å, $b = 12.989$ Å, $c = 22.921$ Å; $\beta = 93.7°$; $Z = 2$; $P2_1/c$. Subsequent X-ray structural and elemental analyses revealed that those crystals contain the anhydrous complex $[(HC(Ph_2PO)_3)_2Cu](ClO_4)_2$; Observed: C, 58.6; H, 4.2. Calculated for $C_{74}H_{62}Cl_2CuO_{14}P_6$: C, 59.4; H, 4.2.

X-ray Crystallography. A single crystal of $[(HC(Ph_2PO)_3)_2Cu](ClO_4)_2 \cdot 2H_2O$ was selected, ground to a sphere of radius 0.40 mm, and mounted in a thin-walled glass capillary. All X-ray diffraction data were collected using graphite monochromated Mo Kα radiation ($\lambda = 0.71073$ Å) on a Nonius Kappa CCD diffractometer fitted with an Oxford model 700 cryostream cooler at 90, 125, 160, 200, 240, 280, 298, 315, and 330 K. Each data set was measured using a combination of φ and ω scans with κ offsets. The data frames were integrated and scaled using the Denzo-SMN package. The structures were solved by direct methods and refined by full-matrix least squares using the software teXsan for Windows v. 1.06. The details of the crystal structure determinations and unit cell parameters for nine temperatures between 90 and 340 K are given in Table 1; a stereoview of the molecule including the atomic labeling scheme is shown in Figure 1.

EPR Measurements. EPR measurements were carried out at Q-band (∼35 GHz) frequency on a powdered sample using a Bruker Elexsys E500 multifrequency continuous wave EPR spectrometer. Low-temperature measurements were performed using the Oxford Instruments CF-935 cryostat in conjunction with an Oxford Instruments ITC-4 temperature controller. The magnetic field was calibrated with a Bruker ER035M gaussmeter, and the microwave frequency was measured with an EIP 548B microwave frequency counter. The spectra were analyzed using the *Xsophe-Sophe-XeprView* computer simulation software suite developed by Hanson et al. that is distributed by Bruker Biospin GmbH.[19]See Figure 2 for experimental spectra and computer simulations.

Results and Discussion

The Cu−O bond distances and angles of the centrosymmetric copper complex at the different temperatures are listed in Table 2. All atomic positions, bond lengths and angles, and thermal parameters are listed in Supporting Information Tables 1−9.

The metal ion sits on an inversion center of the triclinic unit cell, with both tripodal $HC(Ph_2PO)_3$ ligands binding to the copper(II) through three oxygen atoms to form a distorted

(10) Ellis, P. J.; Freeman, H. C.; Hitchman, M. A.; Reinen, D.; Wagner, B. *Inorg. Chem.* **1994**, *33*, 1249.
(11) Riley, M. J.; Hitchman, M. A.; Reinen, D. *Chem. Phys.* **1986**, *102*, 11.
(12) Riley, M. J.; Hitchman, M. A.; Wan Mohammed, A. *J. Chem. Phys.* **1987**, *7*, 3766.
(13) Astley, T.; Headlam, H.; Hitchman, M. A.; Keene, F. R.; Pilbrow, J.; Stratemeier, H.; Tiekink, E.; Zhong, Y. C. *J. Chem. Soc., Dalton Trans.* **1995**, 3809.
(14) Bebendorf, J.; Bürgi, H.-B.; Gamp, E.; Hitchman, M. A.; Murphy, A.; Reinen, D.; Riley, M. J.; Stratemeier, H. *Inorg. Chem.* **1996**, *35*, 7419.
(15) Rauw, W.; Ahsbas, H.; Hitchman, M. A.; Lukin, S.; Reinen, D.; Schultz, A.; Simmons, C. J.; Stratemeier, H. *Inorg. Chem.* **1996**, *35*, 1902.
(16) Hitchman, M. A.; Maaskant, W.; van der Plas, J.; Simmons, C. J.; Stratemeier, H. *J. Am. Chem. Soc.* **1999**, *121*, 1488.
(17) Shieh, S.-J.; Che, C.-M.; Peng, S.-M. *Inorg. Chim. Acta* **1992**, *192*, 151.
(18) Masters, V. M.; Riley, M. J.; Hitchman, M. A.; Simmons, C. J. *Inorg. Chem.* **2001**, *40*, 4478.
(19) (a) Hanson, G. R.; Gates, K. E.; Noble, C. J.; Griffin, M.; Mitchell, A.; Benson, S. *J. Inorg. Biochem.* **2004**, *98*, 903. (b) Wang, D.; Hanson, G. R. *Appl. Magn. Reson.* **1996**, *11*, 401.

Table 1. Crystallographic Data for [(HC(Ph$_2$PO)$_3$)$_2$Cu](ClO$_4$)$_2$·2H$_2$O

	T = 90 K	T = 125 K	T = 160 K	T = 200 K	T = 240 K	T = 280 K	T = 298 K	T = 315 K	T = 330 K
formula					$C_{74}H_{66}Cl_2CO_{16}P_6$				
fw					1531.62				
space group					$P\bar{1}$ (triclinic)				
cryst size, mm					sphere = 0.40				
a (Å)	11.7862(1)	11.8203(1)	11.8559(1)	11.9010(1)	11.9497(1)	11.9994(1)	12.0163(1)	12.0338(1)	12.0557(7)
b (Å)	12.3930(1)	12.3856(1)	12.3697(1)	12.3410(1)	12.3039(2)	12.2868(2)	12.2846(2)	12.2821(2)	12.2875(6)
c (Å)	12.7564(1)	12.8115(2)	12.8743(2)	12.9658(2)	13.0723(2)	13.1556(2)	13.1828(2)	13.2079(2)	13.2161(8)
α (deg)	89.9000(4)	90.0281(4)	90.1433(4)	90.2833(4)	90.4432(5)	90.6621(5)	90.7630(5)	90.8688(5)	90.8771(17)
β (deg)	106.8770(4)	107.2095(7)	107.2222(4)	107.4762(5)	107.7322(5)	107.9433(5)	107.9912(5)	108.0313(5)	108.0608(2)
γ (deg)	98.2690(6)	98.3390 (9)	98.4537 (7)	98.6287(7)	98.8379(8)	99.0123(8)	99.0673(8)	99.1206(10)	99.2748(52)
V (Å^3)	1762.92(2)	1770.84(3)	1781.70(3)	1793.31(3)	1805.91(4)	1818.77(4)	1823.72(4)	1828.50(4)	1832.51(19)
Z					1				
d_{calc} (g cm^{-3})	1.443	1.436	1.427	1.418	1.408	1.398	1.394	1.391	1.388
diffractometer					Nonius kappa CCD X-ray diffractometer				
radiation					Mo Kα (0.71073 Å)				
μ (cm^{-1})					5.8				
reflns measured	28115	28593	28722	27175	28866	29257	19609	15601	6532
indep reflns measured	15350	15468	15535	15703	15822	15937	10661	8356	4595
R_{int}	0.020	0.024	0.025	0.027	0.028	0.024	0.017	0.015	0.031
2θ range	3.3 < 2θ < 69.9	3.3 < 2θ < 69.9	3.3 < 2θ < 69.8	3.3 < 2θ < 69.8	3.3 < 2θ < 70.0	3.3 < 2θ < 70.0	3.3 < 2θ < 60.1	3.3 < 2θ < 55.0	5.3 < 2θ < 55.0
range of h, k, l	±18, ±19, ±20	±18, ±19, ±20	±19, ±19, ±20	±19, ±19, ±20	±19, ±19, ±21	±18, ±19, ±20	±16, ±17, ±18	±15, ±15, ±17	±12, ±15, ±16
reflns (n) used in least squares with $I > 4\sigma(I)$	11671	10231	9859	8914	7806	8583	7398	6282	3394
no. of parameters (p) used in least squares	580	580	580	580	580	580	580	580	580
largest shift/error	0.0	0.18	0.0	0.0	0.0	0.0	0.0	0.0	0.0
R^a	0.039	0.034	0.034	0.037	0.037	0.039	0.040	0.039	0.051
$R_w{}^b$	0.044	0.041	0.043	0.042	0.044	0.048	0.051	0.050	0.059
goodness-of-fit (GOF) on F^c	2.010	1.850	1.920	1.890	2.060	2.340	2.700	2.900	2.250

[a] $R = \sum||F_o| - |F_c||/\sum|F_o|$. [b] $R_w = [\sum w(|F_o| - |F_c|)^2/\sum wF_o^2]^{1/2}$. [c] GOF = $[\sum w(|F_o| - |F_c|)^2/(n - p)]^{1/2}$.

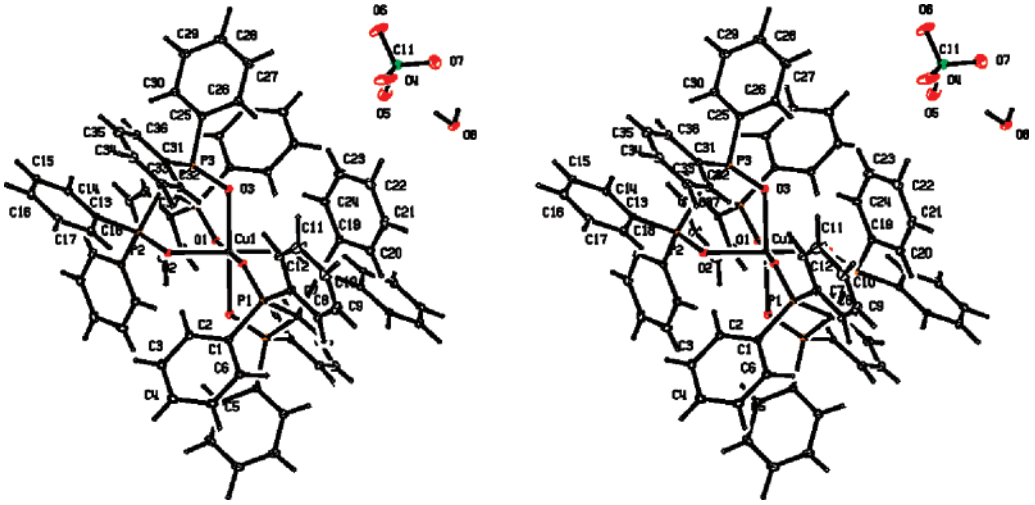

Figure 1. ORTEP stereoview of $[(HC(Ph_2PO)_3)_2Cu](ClO_4)_2 \cdot 2H_2O$ at RT showing the atomic numbering; drawn with ellipsoids of 5% probability. The Cu^{2+} ion sits on a site of inversion symmetry.

Table 2. Selected Bond Lengths (Å) and Angles (deg) for $[(HC(Ph_2PO)_3)_2Cu](ClO_4)_2 \cdot 2H_2O$ at Various Temperatures

temp (K)	Cu−O1 (Å)	Cu−O2 (Å)	Cu−O3 (Å)	O1−Cu−O2 (deg)	O1−Cu−O3 (deg)	O2−Cu−O3 (deg)
90	1.9674(8)	2.0098(8)	2.2952(8)	87.47(3)	93.16(3)	88.24(3)
125	1.9663(12)	2.0216(13)	2.2863(13)	87.48(5)	93.07(6)	88.21(5)
160	1.9675(10)	2.0317(11)	2.2742(10)	87.87(4)	92.88(4)	88.16(4)
200	1.9685(10)	2.0629(12)	2.2401(12)	88.25(4)	92.43(4)	88.15(4)
240	1.9711(12)	2.1045(14)	2.1926(14)	88.77(5)	91.88(5)	87.97(5)
280	1.9753(11)	2.1294(13)	2.1602(13)	89.10(5)	91.50(5)	87.81(5)
298	1.9767(12)	2.1319(15)	2.1570(15)	89.25(5)	91.43(5)	87.85(5)
315	1.9777(13)	2.1375(16)	2.1492(16)	89.29(6)	91.49(6)	87.76(6)
330	1.9790(30)	2.1413(30)	2.1419(27)	89.70(12)	91.25(11)	87.57(10)

octahedral complex. Two water molecules of solvation are present per formula unit. At 298 K the bond lengths and angles of the copper(II) complex are very similar to those reported at 295 K in the previous X-ray structure determination.[17] The distances [1.9767 (×2), 2.1319 (×2), 2.1570 (×2) Å; $T = 298$ K] imply four almost equivalent longer bonds and two shorter bonds, corresponding approximately to the unusual tetragonally compressed stereochemistry. At the higher temperature of 330 K, the four longer bonds become equal within experimental uncertainty (Table 2), so that this coordination geometry becomes essentially regular. However, on cooling to 90 K the longer bond lengths progressively diverge, and one pair approaches the short bonds in length (Table 2) to produce the tetragonally elongated octahedral coordination geometry commonly observed for copper(II).

As shown by EXAFS[18] and discussed in the following section, the longer bond lengths at higher temperatures do not represent the true Cu−O distances in the complex but are the average of two complexes in thermal equilibrium. It might be expected that the disorder in atomic positions produced by this equilibrium would give rise to anomalous thermal parameters for atoms O2 and O3. An examination of the mean-square displacement along the Cu−O bonds, $\Delta U_{obs}(Cu-O)/Å^2$ (Table 3), reveals that the values for all bonds at 90 K, ∼0.002 Å^2, are typical for intramolecular stretching motions.[8] However, the $\Delta U_{obs}(Cu-O)$ values increase nearly 10-fold for the longer Cu−O2 and Cu−O3 bonds and 3-fold for the shorter Cu−O1 bond when going from 90 to 330 K, suggesting some degree of fluxionality. $\Delta U_{obs}(Cu-O)$ values for the longer bonds at 330 K, ∼0.02 Å^2, are similar to those observed for the $(ND_4)_2[Cu(D_2O)_6](SO_4)_2$ and $(NH_4)_2[Cu(H_2O)_6](SO_4)_2$ Tutton salts at 298−321 K,[20] but are far smaller than those observed for the fluxional pseudo-Jahn−Teller $[Cu(phen)_2(CH_3CO_2)]BF_4 \cdot 2H_2O$ and $ClO_4 \cdot 2H_2O$ complexes at room temperature, 0.12 Å^2.[4] Although it might be of interest to compare $\Delta U_{obs}(Cu-O)$ values with those of the isomorphous non-JT zinc(II) analogue of the present complex at different temperatures, repeated attempts to prepare the analogue have been unsuccessful.

Table 3. Mean Square Displacement, ΔU_{obs} (Å^2), along the Copper−Oxygen Bonds for $[(HC(Ph_2PO)_3)_2Cu](ClO_4)_2 \cdot 2H_2O$ at Various Temperatures

	ΔU_{obs} (Å^2)		
temp (K)	Cu−O1	Cu−O2	Cu−O3
90	0.002	0.002	0.002
125	0.002	0.003	0.003
160	0.002	0.006	0.006
200	0.002	0.011	0.012
240	0.002	0.018	0.019
280	0.004	0.020	0.020
298	0.003	0.020	0.021
315	0.005	0.021	0.020
330	0.006	0.021	0.017

Application of the Model of Dynamic JT Coupling to the Thermal Behavior. The model used to describe the potential surface and vibronic energy levels of a copper(II) complex under the influence of JT coupling and a lattice strain has been reported in detail previously.[11,12] For the present complex, the energy of the transition between the

(20) Masters, V. M.; Riley, M. J.; Hitchman, M. A. *Inorg. Chem.* **2001**, *40*, 843.

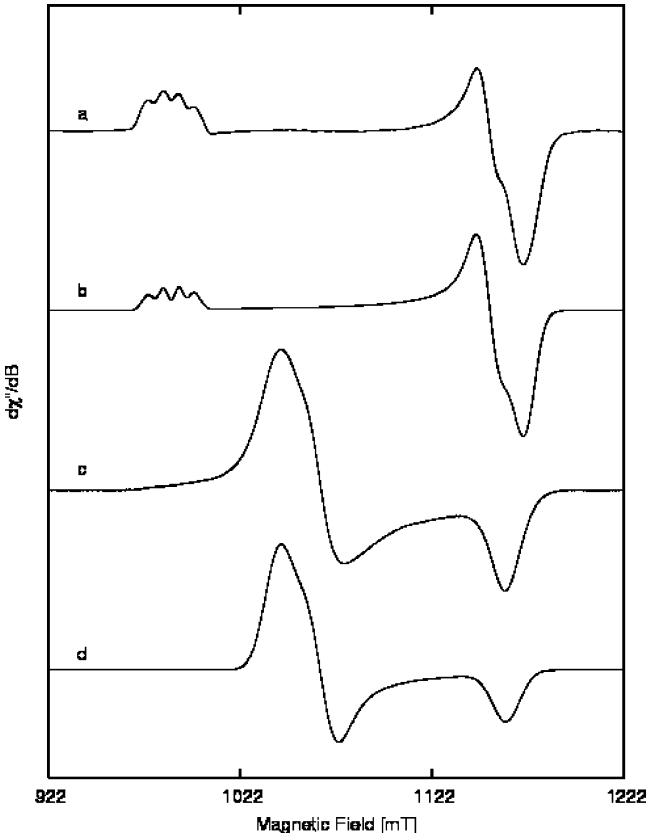

Figure 2. Powder EPR spectra of [(HC(Ph$_2$PO)$_3$)$_2$Cu](ClO$_4$)$_2$·2H$_2$O. (a) Experimental spectrum (33.9831 GHz); $T = 9.1$ K. (b) Computer simulation; $T = 9.1$ K. (c) Experimental spectrum (33.7891 GHz); $T = 292.0$ K. (d) Computer simulation; $T = 292.0$ K.

split components of the E_g state could not be observed spectroscopically, so this could not be used in the estimation of the JT parameters.[12,13] Values for the linear and higher-order JT constants, A_1 and A_2, and the energy of the JT-active vibration, ν, similar to those reported for the [Cu(H$_2$O)$_6$]$^{2+}$ ion[12] and the complex [Cu(tos)$_2$](ClO$_4$)$_2$ (where tos is the tripod ligand 1,3,5-trihydroxycyclohexane)[14] were therefore used as initial estimates for the present compound. It was found that the Cu−O bond distances and the molecular g-values observed at low temperature for [(HC(Ph$_2$PO)$_3$)$_2$Cu](ClO$_4$)$_2$·2H$_2$O could be reproduced satisfactorily using quite similar parameters: $A_1 = 875$, $A_2 = 40$ ($\beta = 340$), and $\nu = 300$, all in cm^{-1}. An atomic mass of 16 amu was used in the calculations; given the polyatomic nature of the ligand, it must be noted that this and the energy ν are "effective" rather than realistic values, as was also recognized in the treatment of [Cu(tos)$_2$](ClO$_4$)$_2$.[14] The orbital reduction parameters $k_x = 0.77$, $k_y = 0.73$, and $k_z = 0.74$ were used to estimate the g-values; these parameters basically act as scaling factors and lie in the lower range of those observed for similar systems.[12−15]

The temperature dependence of the bond lengths and g-values, as shown in Figure 3, is strongly influenced by the lattice strain acting on the complex. This is parametrized by the axial and orthorhombic components S_θ and S_ϵ. While these do not act completely independently, the former mainly influences the orthorhombicity of the complex and the temperature dependence of the lowest g-value and bond

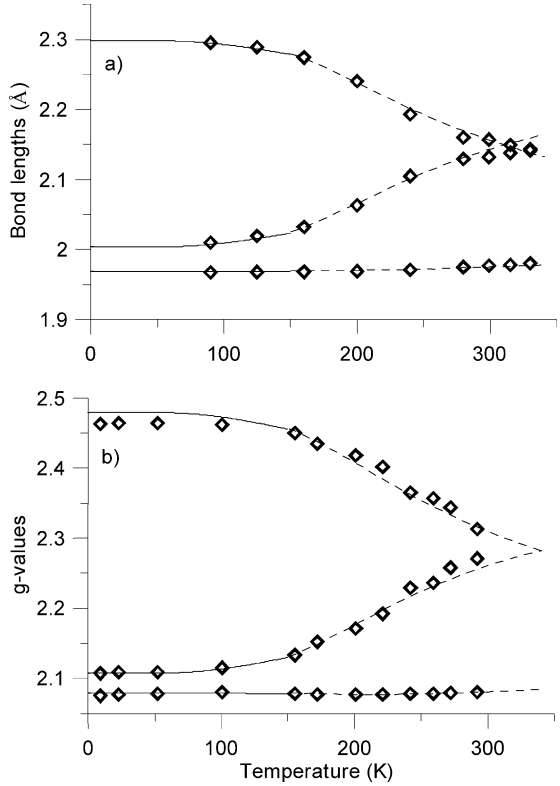

Figure 3. Temperature dependence of (a) the bond lengths and (b) the principal g-values. Values calculated using an orthorhombic strain $S_\epsilon = 170$ cm^{-1} are shown as full lines, while values calculated using an orthorhombic strain which decreases to 1 cm^{-1} between 150 and 340 K (see Figure 4) are shown as dashed lines.

length.[12−15] The fact that these do not change below 340 K places a firm lower limit on S_θ, and a value of -400 cm^{-1} for this parameter was found to be consistent with the data. (The negative sign indicates that the strain is a compression.[12]) The orthorhombic component of the strain is the main factor which decides the thermal behavior of the two higher bond lengths and g-values, and the data below 150 K suggest the value $S_\epsilon = 170$ cm^{-1}, as indicated by the full lines in Figure 3. However, above 150 K the bond lengths and g-values converge much more rapidly than predicted by the model. This implies a decrease in the orthorhombic component of the strain as the temperature rises from 150 to 340 K, and the values of S_ϵ that give optimum agreement with the bond lengths, assuming all other parameters do not change with temperature, are shown in Figure 4. The bond lengths and g-values may be explained satisfactorily over the whole temperature range on this basis, as the dashed lines in Figure 3 indicate. It should be noted that a small change in S_θ with temperature cannot be ruled out. Because S_θ is much larger than S_ϵ , a small change would have a minimal effect on the g-values and bond lengths. However, a significant decrease of ∼100 cm^{-1} or more in S_θ can be ruled out, as this would cause the lowest g-value and bond lengths to increase, which is not observed experimentally.

Interpretation of the JT and Lattice Strain Parameters. The overall JT distortion radius, R_{JT}, is defined conventionally[1] as

$$R_{JT} = [2(d_x)^2 + 2(d_y)^2 + 2(d_z)^2]^{1/2}$$

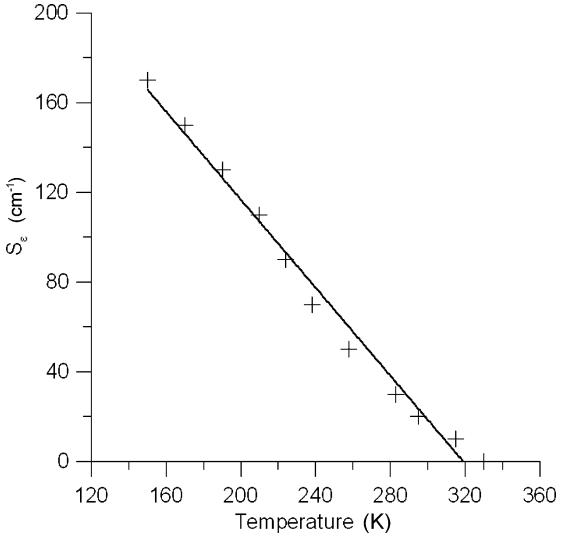

Figure 4. Values of S_ϵ that give optimum agreement with the observed bond lengths and *g*-values at various temperatures.

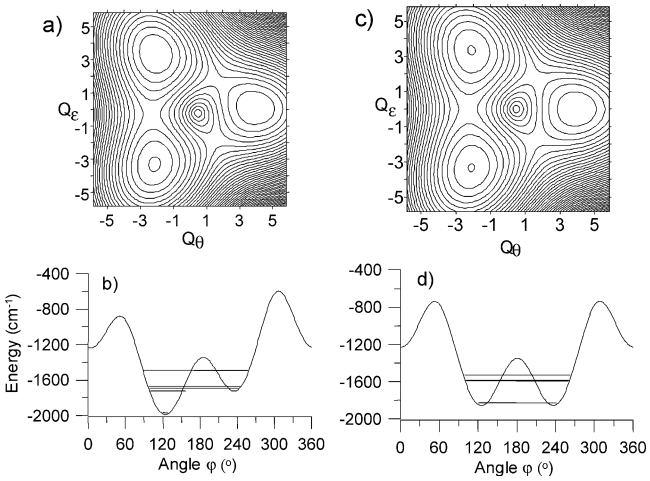

Figure 5. Contour energy plots and radial energy curves for the complexes with the orthorhombic strains $S_\epsilon = 170$ cm^{-1} (a and b, respectively) and $S_\epsilon = 1$ cm^{-1} (c and d, respectively); see text for the values of the other parameters and the method of calculation.

and the bond lengths observed at low temperature for the complex $[(HC(Ph_2PO)_3)_2Cu](ClO_4)_2 \cdot 2H_2O$ imply the value $R_{JT} = 0.36$ Å. This is in the range 0.33−0.39 Å observed for the $[Cu(H_2O)_6]^{2+}$ ion in the $X_2[Cu(H_2O)_6](YO_4)_2$ Tutton salts (X = monovalent cation; M = Cu^{2+}; Y = S or Se)[15] and is somewhat larger than the distortion of 0.271 Å seen for the complex $[Cu(tos)_2]^{2+}$.[14] Evidently the $(HC(Ph_2PO)_3)$ ligand is sufficiently flexible that it does not significantly inhibit distortion of the copper(II) complex.

The JT parameters defining the potential surface of the complex below 150 K are quite similar to those of other complexes exhibiting dynamic JT behavior.[12−15] A contour plot of the potential surface of the $[(HC(Ph_2PO)_3)_2Cu]^{2+}$ ion in this temperature range is shown in Figure 5a, and the change in energy as a function of the coordination geometry at the JT radius of the minimum is shown in Figure 5b. The energies of the six lowest vibronic wave functions are indicated in the latter, and the Cu−O distances and *g*-values associated with these are shown in Table 4. As for other

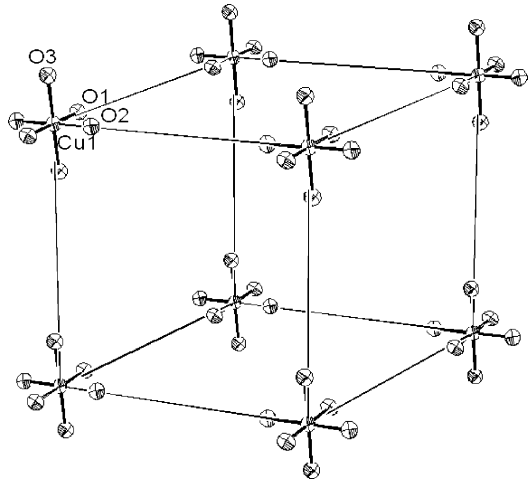

Figure 6. Molecular packing of the complex showing the ferrodistortive arrangement of the Cu−O bonds; i.e., the crystallographically equivalent Cu−O bonds of adjacent complexes are parallel with respect to each other, rather than perpendicular as for an antiferrodistortive arrangement.

Table 4. *g*-Values and Bond Lengths for the Sixth-Lowest Energy Levels of the Low-Temperature and High-Temperature Potential Surfaces

strain (S_ϵ; cm^{-1})	energy (cm^{-1})	g_x	g_y	g_z	d_x (Å)	d_y (Å)	d_z (Å)
170	0	2.4668	2.1075	2.0796	2.2982	2.0036	1.9682
	246	2.4638	2.1167	2.0729	2.2945	2.009	1.9665
	271	2.1365	2.424	2.0676	2.0266	2.2783	1.9652
	300	2.4643	2.1056	2.0839	2.2933	2.005	1.9718
	476	2.4021	2.1944	2.0516	2.2378	2.0696	1.9626
	505	2.2205	2.3543	2.0596	2.0918	2.2152	1.9630
1	0	2.4752	2.1168	2.0731	2.2860	2.0173	1.9667
	1	2.1349	2.422	2.0741	2.0174	2.2859	1.9667
	237	2.3449	2.2463	2.0604	2.1790	2.1269	1.9641
	244	2.2766	2.3023	2.0660	2.1269	2.1786	1.9645
	300	2.4348	2.1478	2.0786	2.2522	2.0473	1.9705
	302	2.1694	2.3857	2.0795	2.0475	2.2521	1.9704

similar complexes, the potential surface has three well-defined minima, the two lowest being rather close in energy. Inspection of the bond lengths and *g*-values (Table 4) shows that the wave functions are strongly localized in the lower pair of minima. For the first and third wave functions, although the magnitudes of the bond lengths and *g*-values are similar, the values along the *x* and *y* axes are interchanged (*z* is defined to lie along the direction of the axial component of the lattice strain). As originally recognized by Silver and Getz,[21] and subsequently confirmed by later workers,[4,12] it is the thermal population of this upper wave function that causes the characteristic temperature dependence of the two lower *g*-values and bond lengths of complexes exhibiting this kind of dynamic JT effect. To a first approximation, the second, fourth, and fifth wave functions are higher vibrational states of the lowest wave function, while the sixth is the first excited vibrational state of the third wave function. The wave functions that are localized largely in the highest minimum are too high in energy to be thermally populated at the highest temperature available.

Above 150 K, the temperature dependence departs from Boltzmann behavior and implies a steady, almost linear

(21) Silver, B. L.; Getz, D. *J. Chem. Phys.* **1974**, *61*, 638.

decrease in the orthorhombic component of the lattice strain until by 340 K this has become negligible (Figure 4). The contour plot and radial energy curve appropriate to a value of $S_\epsilon = 1$ cm^{-1} are shown in Figure 5c and d. The results are insensitive to the precise value of S_ϵ within the range $10 < S_\epsilon < 0.1$ cm^{-1}. (Note that random strains of this order of magnitude are likely to be present in the lattice in addition to those due to the crystal packing.[22]) The contour plot shows that in *absolute* terms the potential surface is not dramatically different from that below 150 K. The radial energy plot (Figure 5d) shows two essentially equivalent minima, separated by a significant saddle point. The high-energy barrier and small residual orthorhombic strain mean that the bond lengths and *g*-values of the two lowest wave functions (Table 4) remain localized, one in each well. Because the energy separation between them is so small, they are essentially equally populated and the bond lengths and *g*-values are averaged. The potential surface at this temperature is rather similar to that of the complex [Cu(H$_2$O)$_2$Cl$_4$]$^{2-}$ in Cu^{2+}-doped NH$_4$Cl, which has been discussed in detail elsewhere.[22] Here, the two lowest wave functions correspond to complexes that have short bonds to the water molecules and short and long bonds to different pairs of chloride ions. In this case the lattice is cubic, and the long and short Cu−Cl bonds are discriminated solely by random lattice strains. It must be stressed that although the strain, macroscopic bond lengths, and *g*-values of these complexes are all close to axially symmetric, at the molecular level the copper(II) complexes have an orthorhombically distorted geometry. The situation is thus quite different from that inferred, for instance, for the analogous complex [Cu(NH$_3$)$_2$Cl$_4$]$^{-2}$ in Cu^{2+}-doped NH$_4$Cl, where the stronger axial compression produces a complex with a true, tetragonally compressed geometry.[22]

It is of interest to consider why the orthorhombic component of the lattice strain in [(HC(Ph$_2$PO)$_3$)$_2$Cu](ClO$_4$)$_2$·2H$_2$O decreases as the temperature rises from 150 to 340 K. Similar behavior has been observed for other "dynamic" Cu^{2+} compounds, most notably (NH$_4$)$_2$[Cu(H$_2$O)$_6$](SO$_4$)$_2$ and its deuterated analogue.[16,23] Here, the two longer Cu−O bonds and the higher *g*-values also converge, though over a narrower temperature range, 220−315 K. It has been suggested that in this case the deviation from Boltzmann behavior may be caused by cooperative interactions between the copper(II) complexes.[16] In this process, when one copper(II) complex is thermally excited, the change in geometry produces a strain which lowers the excitation energy of its neighbors; a simple model based on this concept explained the observed behavior.[16] This model predicts that at high temperature the potential surface of each copper(II) complex will depend on the geometry of its neighbors and that the thermally excited complexes will tend to cluster to form domains.[16] However, it seems unlikely that direct cooperative interactions of this kind occur in [(HC(Ph$_2$PO)$_3$)$_2$Cu](ClO$_4$)$_2$·2H$_2$O. First, the bulky nature of the ligand should "cushion" the effects produced by a change in the direction of the JT distortion. No evidence for cooperative effects was observed for the compound [Cu(tos)$_2$](ClO$_4$)$_2$, and indeed this bulky ligand was specifically chosen to minimize the likelihood of such interactions.[14] Second, unlike the case of (ND$_4$)$_2$[Cu(D$_2$O)$_6$](SO$_4$)$_2$, where the [Cu(D$_2$O)$_6$]$^{2+}$ ions stack in an antiferrodistortive pattern,[24] the complexes in [(HC(Ph$_2$PO)$_3$)$_2$Cu](ClO$_4$)$_2$·2H$_2$O stack in a ferrodistortive manner (Figure 6). As the nature of cooperative interactions of the above kind depends on the packing arrangement,[16] the ferrodistortive packing should *enhance*, rather than reduce, the orthorhombic strain in the latter compound.[25]

It thus seems likely that the thermal behavior of [(HC(Ph$_2$PO)$_3$)$_2$Cu](ClO$_4$)$_2$·2H$_2$O is simpler than that proposed for (NH$_4$)$_2$[Cu(H$_2$O)$_6$](SO$_4$)$_2$,[16] with the potential surface of each complex changing smoothly from that shown in Figure 5a and b to that shown in Figure 5c and d as the temperature rises from 90 to 150 K. There are no specific pointers to this in the hydrogen-bonding interaction, so it seems likely that the decrease in S_ϵ simply reflects the general loosening of the intermolecular contacts accompanying the rise in temperature. Although behavior of this kind is not shown by most dynamic copper(II) complexes, when deviations from Boltzmann behavior do occur, they generally result from structural changes which cause the lattice strain to become more isotropic. This is the case for Cs$_2$[Cu(H$_2$O)$_6$]ZrF$_6$, both in the pure state[26] and for Cu^{2+} doped into the corresponding zinc(II) compound.[27] Similarly, the lattice strain in the compound CuCrO$_4$ alters from orthorhombic to tetragonal on going from low to high temperature, though this is accompanied by a phase change.[28]

The fact that cooperative interactions cannot be responsible for the unusual behavior of [(HC(Ph$_2$PO)$_3$)$_2$Cu](ClO$_4$)$_2$·2H$_2$O raises the question of whether such interactions are indeed the cause of the similar behavior of (NH$_4$)$_2$[Cu(H$_2$O)$_6$](SO$_4$)$_2$. Indeed, Augustyniak and Usachev[29] have proposed that it is changes in the librations of the ammonium groups that influence the orthorhombic lattice strain parameter and hence the thermal properties of the latter compound. In our view, the role of cooperative interactions and lattice forces in the Tutton salts remains an open question that warrants further study.

Conclusions

The temperature dependence of the Cu−O bond lengths and molecular *g*-values of [(HC(Ph$_2$PO)$_3$)$_2$Cu](ClO$_4$)$_2$·2H$_2$O shows that the tetragonally compressed octahedral geometry observed for the copper(II) complex at high temperature is

(22) Riley, M. J.; Hitchman, M. A.; Reinen, D.; Steffen, G. *Inorg. Chem.* **1988**, *27*, 1924.
(23) Augustyniak, M. A.; Krupski, M. *Chem. Phys. Lett.* **1999**, *311*, 126.
(24) Reinen, D.; Friebel, C. *Struct. Bonding (Berlin)* **1979**, *37*, 1.
(25) See ref 16 for a detailed account of the influence of crystal packing on the cooperative interaction.
(26) Augustyniak-Jablokow, M. A.; Krupska, A.; Krupski, M.; Yablokov, Y. V. *Inorg. Chem.* **2002**, *41*, 1348.
(27) Hitchman, M. A.; Yablokov, Y. V.; Petrashen, V. E.; Augustyniak-Jablokow, M. A.; Stratemeier, H.; Riley, M. J.; Lukaszewicz, K.; Tomaszewski, P. E.; Pietraszko, A. *Inorg. Chem.* **2002**, *41*, 229.
(28) Headlam, H.; Hitchman, M. A.; Stratemeier, H.; Smits, J. M. M.; Beurskens, P. T.; de Boer, E.; Janssen, G.; Gatehouse, B. M.; Deacon, G.; Ward, G. N.; Riley, M. J.; Wang, D. *Inorg. Chem.* **1995**, *34*, 5516.
(29) Augustyniak, M. A.; Usachev, A. E. *J. Phys. C* **1999**, *11*, 4391.

due to a thermal equilibrium between structural forms having slightly distorted tetragonally elongated geometries, but with the long bonds to different pairs of oxygen atoms. The potential surface and vibronic wave functions of the complex have been calculated by considering the effects of JT coupling and lattice strain interactions. However, agreement with experiment is obtained only if the orthorhombic component of the strain decreases to a negligible value as the temperature rises to 340 K. The specific change in the lattice which causes this transformation in the strain acting upon the copper(II) complex has not been identified, but it seems unlikely that it is due to direct cooperative interactions between neighboring complexes.

Acknowledgment. Financial assistance from the Australian Research Commission is acknowledged by M.A.H., H.S., and G.R.H.

Supporting Information Available: Additional information on data collection and experimental details; tables including all atomic positions, bond lengths and angles, and thermal parameters. This material is available free of charge via the Internet at http://pubs.acs.org.

IC048604H